

# Can black-hole neutrino-cooled disks power short gamma-ray bursts?

Tong Liu<sup>1,2,3,4,\*</sup>, Yi-Qing Lin<sup>5</sup>, Shu-Jin Hou<sup>6,2</sup>, Wei-Min Gu<sup>1,4</sup>

\*tongliu@xmu.edu.cn

## ABSTRACT

Stellar-mass black holes (BHs) surrounded by neutrino-dominated accretion flows (NDAFs) are the plausible candidates to power gamma-ray bursts (GRBs) via neutrinos emission and their annihilation. The progenitors of short-duration GRBs (SGRBs) are generally considered to be compact binaries mergers. According to the simulation results, the disk mass of the NDAF has been limited after merger events. We can estimate such disk mass by using the current SGRB observational data and fireball model. The results show that the disk mass of a certain SGRB mainly depends on its output energy, jet opening angle, and central BH characteristics. Even for the extreme BH parameters, some SGRBs require massive disks, which approach or exceed the limits in simulations. We suggest that there may exist alternative magnetohydrodynamic processes or some mechanisms increasing the neutrino emission to produce SGRBs with the reasonable BH parameters and disk mass.

*Subject headings:* accretion, accretion disks - black hole physics - gamma-ray burst: general - neutrinos

---

<sup>1</sup>Department of Astronomy and Institute of Theoretical Physics and Astrophysics, Xiamen University, Xiamen, Fujian 361005, China

<sup>2</sup>Key Laboratory for the Structure and Evolution of Celestial Objects, Chinese Academy of Sciences, Kunming, Yunnan 650011, China

<sup>3</sup>State Key Laboratory of Theoretical Physics, Institute of Theoretical Physics, Chinese Academy of Sciences, Beijing 100190, China

<sup>4</sup>SHAO-XMU Joint Center for Astrophysics, Xiamen University, Xiamen, Fujian 361005, China

<sup>5</sup>School of Opto-electronic and Communication Engineering, Xiamen University of Technology, Xiamen, Fujian 361024, China

<sup>6</sup>College of Physics and Electronic Engineering, Nanyang Normal University, Nanyang, Henan 473061, China

## 1. Introduction

Gamma-ray bursts (GRBs) are the most powerful electromagnetic events in the universe, which are sorted into two categories, i.e., short- and long-duration GRBs (SGRBs and LGRBs, see Kouveliotou et al. 1993) or type I and II GRBs (Zhang 2006; Zhang et al. 2007a). Their progenitors are considered to be mergers of two compact objects, i.e., two neutron stars (NSs) or a black hole (BH) and a NS (for reviews, see, e.g., Nakar 2007; Berger 2014), and collapses of massive stars (e.g., Woosley & Bloom 2006 for reviews), respectively. For the interpretations on the gamma-ray and afterglow emission of GRBs, the fireball shock model (for reviews, see, e.g., Mészáros 2002; Zhang & Mészáros 2004) has been widely accepted. The popular models on the central engines of GRBs are either a rotating stellar BH surrounded by a hyperaccretion disk (e.g., Paczyński 1991; Narayan et al. 1992; MacFadyen & Woosley 1999) or a quickly rotating magnetar (or protomagnetar, e.g., Usov 1992; Metzger et al. 2011; Lü et al. 2015).

Two mechanisms have been proposed to power GRBs if a hyperaccretion disk exists in the center of GRBs, i.e., neutrino emission and annihilation, and magnetohydrodynamic processes, such as Blandford-Znajek (BZ) mechanism (Blandford & Znajek 1977) and episodic magnetic reconnection (Yuan & Zhang 2012). For the former mechanism, neutrino annihilation can produce a relativistic electron-positron outflow, which is considered as the progenitor of the fireball to power a GRB. The most probable model to launch a large number of neutrinos is a geometrically and optically thick neutrino-cooled hyperaccretion disks, named as neutrino-dominated accretion flow (NDAF), whose typical characteristics are extremely high accretion rate and neutrino-cooling process. In the inner region of the NDAF, the main components are the electrons, free neutrons and protons, the density and temperature are very high ( $\rho \sim 10^{10} - 10^{13} \text{ g cm}^{-3}$  and  $T \sim 10^{10} - 10^{11} \text{ K}$ ), and the photons are tightly trapped in such disk, thus the energy loss is mainly through neutrino and antineutrino radiation (see, e.g., Popham et al. 1999; Di Matteo et al. 2002; Kohri & Mineshige 2002; Rosswog & Ramirez-Ruiz 2002; Kohri et al. 2005; Lee et al. 2005; Gu et al. 2006; Chen & Beloborodov 2007; Liu et al. 2007; Kawanaka & Mineshige 2007; Zalamea & Beloborodov 2011; Janiuk et al. 2013; Kawanaka et al. 2013; Xue et al. 2013).

Two factors should be considered in the calculation of the neutrino luminosity and annihilation luminosity, which are the structure and components of the NDAF and the description of the relativistic neutrino propagation. Xue et al. (2013) investigated the global solutions of the radial structure and components of the NDAF in the Kerr space-time of the BH with detailed neutrino physics and nucleosynthesis processes. The results show that the gas pressure and the neutrino cooling are always dominant in the inner region for the high mass accretion rate, and the major components of the inner, middle, and outer regions are

the free nucleons,  ${}^4\text{He}$ , and  ${}^{56}\text{Fe}$ , respectively. Importantly, they noticed that the radiative neutrinos mainly come from the inner region of the disk, and the neutrino emission rate less depends on the description of the microphysics, as well as other studies of NDAF model (e.g., Popham et al. 1999; Di Matteo et al. 2002; Liu et al. 2007; Kawanaka et al. 2013). Even for the discussions on the vertical structure of the NDAF, the similar solutions are presented (e.g., Liu et al. 2008, 2010, 2012a, 2013, 2014). Thus the main problem is how to precisely calculate the neutrino annihilation processes. Birkel et al. (2007), Kovács et al. (2011a), and Kovács & Harko (2011b) analyzed the influence of general relativistic effects on the neutrino annihilation efficiency, which has a prominent increase compared with the Newtonian calculations. Based on the geodesic-tracing method, Zalamea & Beloborodov (2011) also studied annihilations via tracing the neutrino track.

For SGRBs, Eichler et al. (1989) proposed that the mergers of two NSs might be the candidates. Ruffert & Janka (1998) simulated three-dimensional Newtonian hydrodynamical solutions of the merger events of two NSs with mass  $\sim 1.6 M_{\odot}$ . There might survive a disk  $\sim 0.1 - 0.2 M_{\odot}$  surrounding a BH  $\sim 2.5 M_{\odot}$ . Furthermore, Paczyński (1991) and Narayan et al. (1992) presented that the merger of a NS and a stellar-mass BH can also produce a SGRB. In simulations, the fragments of the NS can form a more massive disk,  $\sim 0.5 M_{\odot}$  (e.g., Kluźniak & Lee 1998; Lee & Kluźniak 1999; Popham et al. 1999; Liu et al. 2012b). In the past several years, the massive NSs, i.e.,  $\sim 2 M_{\odot}$  have been discovered in binaries, which accompany the white dwarfs (Demorest et al. 2010; Antoniadis et al. 2013). Yet we cannot neglect the possibilities that the massive NSs exist in the BH-NS or two NSs binaries. However, the mass of the disk is still much smaller than  $1 M_{\odot}$  with the logical conjecture. So it begs a question: can annihilations of neutrinos from NDAFs owning such disk masses power all the observed SGRBs? Fan & Wei (2011) investigated the disk mass in the center of SGRBs with the fixed values of the BH mass and spin. They found that nearly half SGRBs are suitable for the results of the above simulations. We further consider that the annihilation description, intact samples with prompt emission and afterglow properties of SGRBs, and reasonable ranges of the BH parameters should be fully included to answer the above question.

In Section 2, we describe the physical processes from the neutrino annihilation to observational gamma-ray photons. By using the current SGRBs data, the disk masses for the definite ranges of the BH parameters are shown in Section 3. Conclusions and discussion are in Section 4.

## 2. Model

The neutrino annihilation luminosity  $L_{\nu\bar{\nu}}$  is a function of the BH mass  $M_{\text{BH}}$ , dimensionless spin parameter  $a_*$  ( $a_* \equiv cJ/GM_{\text{BH}}^2$ ,  $J$  is the angular momentum of the BH), dimensionless viscosity parameter  $\alpha$ , and mass accretion rate  $\dot{M}$  (see, e.g., Popham et al. 1999; Rosswog et al. 2003; Gu et al. 2006; Liu et al. 2007; Zalamea & Beloborodov 2011; Kawanaka et al. 2013; Xue et al. 2013; Leng & Giannios 2014).

The analytical formula of  $L_{\nu\bar{\nu}}$  is shown in many previous works (e.g., Fryer et al. 1999; Zalamea & Beloborodov 2011; Xue et al. 2013). Here we adopt the neutrino annihilation luminosity  $L_{\nu\bar{\nu}}$  given by Zalamea & Beloborodov (2011), which is expressed as

$$L_{\nu\bar{\nu}} \approx 5.7 \times 10^{52} x_{\text{ms}}^{-4.8} (M_{\text{BH}}/M_{\odot})^{-3/2} \times \left\{ \begin{array}{ll} 0 & \text{for } \dot{M} < \dot{M}_{\text{ign}} \\ (\dot{M}/M_{\odot} \text{ s}^{-1})^{9/4} & \text{for } \dot{M}_{\text{ign}} < \dot{M} < \dot{M}_{\text{trap}} \\ (\dot{M}_{\text{trap}}/M_{\odot} \text{ s}^{-1})^{9/4} & \text{for } \dot{M} > \dot{M}_{\text{trap}} \end{array} \right\} \text{ erg s}^{-1}, \quad (1)$$

where  $x_{\text{ms}} = r_{\text{ms}}/r_{\text{g}}$ ,  $r_{\text{ms}}$  is radius of the last (marginally stable) orbit,  $r_{\text{g}} = 2GM_{\text{BH}}/c^2$  is the Schwarzschild radius, and  $\dot{M}_{\text{ign}}$  is the critical ignition accretion rate,  $\dot{M}_{\text{trap}}$  is the accretion rate if neutrino trapping events occur in the inner region of the NDAF (e.g., Di Matteo et al. 2002; Kohri et al. 2005; Chen & Beloborodov 2007; Liu et al. 2012a; Xue et al. 2013). Their numerical results depend on the viscosity parameter  $\alpha$  and BH spin parameter  $a_*$ . Additionally, the value of viscosity parameter  $\alpha$  has little effects on  $L_{\nu\bar{\nu}}$  as long as  $\dot{M}_{\text{ign}} < \dot{M} < \dot{M}_{\text{trap}}$  (Zalamea & Beloborodov 2011), so  $\alpha = 0.1$  is adopted here. Furthermore,  $x_{\text{ms}}$  can be expressed as (e.g., Bardeen et al. 1972; Kato et al. 2008; Hou et al. 2014)

$$x_{\text{ms}} = \frac{1}{2}[3 + Z_2 - \sqrt{(3 - Z_1)(3 + Z_1 + 2Z_2)}], \quad (2)$$

where

$$Z_1 = 1 + (1 - a_*^2)^{1/3}[(1 + a_*)^{1/3} + (1 - a_*)^{1/3}], \quad (3)$$

$$Z_2 = \sqrt{3a_*^2 + Z_1^2}. \quad (4)$$

In comparison, Xue et al. (2013) also gave a similar analytical solution, i.e.,  $L_{\nu\bar{\nu}} \propto \dot{M}^{2.17}$ , but the influence of the BH mass was not considered.

Popham et al. (1999) and Liu et al. (2007) investigated the spatial distribution of neutrino annihilation rate and found that nearly 60% of the total annihilation luminosity is ejected from the region  $r < 20 r_{\text{g}}$ . In the studies on the vertical structure of NDAF model

(e.g., Liu et al. 2010, 2012a, 2013), we found that the half-opening angle of the disk is very large,  $\gtrsim 80^\circ$ , for the typical accretion rate,  $\sim 1 M_\odot \text{ s}^{-1}$ , thus the empty funnel along the rotation axis above the disk can naturally limit the opening angle of the neutrino annihilable ejection to produce the primary fireball.

The fireball mean power outputting from the central engine  $\dot{E}$  is a fraction of  $L_{\nu\bar{\nu}}$ , i.e.,

$$\dot{E} = \eta L_{\nu\bar{\nu}}, \quad (5)$$

where  $\eta$  is the conversion factor (e.g., Aloy et al. 2005; Fan & Wei 2011; Liu et al. 2012b). The output power can be written as

$$\dot{E} \approx \frac{(1+z)(E_{\gamma,\text{iso}} + E_{\text{k,iso}})\theta_j^2}{2T_{90}}, \quad (6)$$

where  $z$  is the redshift,  $E_{\gamma,\text{iso}}$  is the isotropic radiated energy in the prompt emission phase,  $E_{\text{k,iso}}$  is the isotropic kinetic energy of the outflow powering long-lasting afterglow,  $T_{90}$  can roughly be considered as the duration of the activity of the central engine, and  $\theta_j$  is the opening angle of the ejecta.

Hence, for the cases of  $\dot{M}_{\text{ign}} < \dot{M} < \dot{M}_{\text{trap}}$ , we have the mean accretion rate (Fan & Wei 2011)

$$\dot{M} \approx 0.12 \left[ \frac{(1+z)(E_{\gamma,\text{iso},51} + E_{\text{k,iso},51})\theta_j^2}{\eta T_{90,s}} \right]^{4/9} x_{\text{ms}}^{2.1} \left( \frac{M_{\text{BH}}}{M_\odot} \right)^{2/3} M_\odot \text{ s}^{-1}, \quad (7)$$

where  $E_{\text{k,iso},51} = E_{\text{k,iso}}/(10^{51} \text{ ergs})$ ,  $E_{\gamma,\text{iso},51} = E_{\gamma,\text{iso}}/(10^{51} \text{ ergs})$ , and  $T_{90,s} = T_{90}/(1 \text{ s})$ . Furthermore, the disk mass is

$$M_{\text{disk}} \approx 0.12 \left[ \frac{(E_{\gamma,\text{iso},51} + E_{\text{k,iso},51})\theta_j^2}{\eta} \right]^{4/9} \left( \frac{T_{90,s}}{1+z} \right)^{5/9} x_{\text{ms}}^{2.1} \left( \frac{M_{\text{BH}}}{M_\odot} \right)^{2/3} M_\odot. \quad (8)$$

According to the above equation, we can estimate the disk mass by using the observational data. It should be noted that there exist some uncertainties, especially for the efficiency  $\eta$  and the interval of the activity of central engine replaced by  $T_{90}$ . There should exist an efficiency from the neutrino annihilation to the initial fireball, then to the jet kinetic energy and radiation, which is mainly related to the energy, components, and state of the fireball (e.g., Eichler et al. 1989; Aloy et al. 2005). Aloy et al. (2005) mentioned that the duration of the GRB event might be longer than the time interval of the activity of central engine if the radial expansion of the fireball is considered. In the fireball model, it is difficult to estimate the duration of such an expansion to the optically thin phase by the observational data unless the blackbody component can be observed. It is conceivable that

the consequences of the use of  $\eta$  and  $T_{90}$  would change the resulting disk mass to some extent although the exponents of  $\eta$  and  $T_{90}$  in Equation (8) are small.

$E_{\gamma,\text{iso}}$  can be calculated by the observational data, which is written as

$$E_{\gamma,\text{iso}} = 4\pi D_L^2 F_\gamma / (1+z), \quad (9)$$

where  $D_L$  is the luminosity distance, and  $F_\gamma$  is the fluence in the 15-150 keV for *Swift* events. Then  $D_L$  is defined as

$$D_L = \frac{(1+z)c}{H_0} \int_0^z [\Omega_M(1+z')^3 + \Omega_\Lambda]^{-1/2} dz', \quad (10)$$

here we employ a standard  $\Lambda$ CDM cosmology model with  $\Omega_M = 0.27$ ,  $\Omega_\Lambda = 0.73$ , and  $H_0 = 71 \text{ km s}^{-1} \text{ Mpc}^{-1}$ . Moreover, the mean isotropic gamma-ray luminosity is

$$L_{\gamma,\text{iso}} \approx E_{\gamma,\text{iso}}(1+z)/T_{90}. \quad (11)$$

$E_{k,\text{iso}}$  and  $\theta_j$  can be deduced from the modeling of the X-ray afterglow data. We take  $E_{k,\text{iso}}$  as (Lloyd-Ronning & Zhang 2004; Fan & Piran 2006; Zhang et al. 2007b)

$$\begin{aligned} E_{k,\text{iso}} \approx & 9.2 \times 10^{52} R L_{X,46}^{4/(p+2)} \left(\frac{1+z}{2}\right)^{-1} \epsilon_{B,-2}^{(2-p)/(p+2)} \epsilon_{e,-1}^{4(1-p)/(p+2)} \\ & \times t_d^{(3p-2)/(p+2)} (1+Y)^{4/(p+2)} \text{ ergs}, \end{aligned} \quad (12)$$

where  $R \sim (t_{11}/T_{90,s})^{17\epsilon_e/16}$  is a factor that accounts for the energy loss during the deceleration following the prompt gamma-ray emission phase (e.g., Sari 1997; Lloyd-Ronning & Zhang 2004),  $\epsilon_{e,0.1} = \epsilon_e/0.1$  is the fractions of shock energy given to the electrons,  $\epsilon_{B,0.1} = \epsilon_B/0.01$  is the fraction of energy in the magnetic field,  $t_{11} = t/(11 \text{ hours})$  and  $t_d = t/(1 \text{ day})$  are the time of observation,  $Y$  is Compton parameter,  $p$  is the energy distribution index of the shock-accelerated electrons and can be fitted by the observed photon index in the X-ray spectrum (e.g., Zhang et al. 2006; Gao et al. 2013), and  $L_{X,46} = L_X/(10^{46} \text{ erg s}^{-1})$  is the isotropic X-ray afterglow luminosity. Here we take the X-ray luminosity at 11 hours since the burst triggers, which can be written as

$$L_X = 4\pi D_L^2 F_X, \quad (13)$$

where  $F_X$  is the X-ray flux of the afterglow recorded by satellites.

Furthermore, the relation between the opening angle and the jet break time is given by (e.g., Sari et al. 1999; Frail et al. 2001; Fong et al. 2012)

$$\theta_j \approx 0.076 \left(\frac{t_j}{1 \text{ day}}\right)^{3/8} \left(\frac{1+z}{2}\right)^{-3/8} \left(\frac{n}{0.01 \text{ cm}^{-3}}\right)^{1/8} E_{k,\text{iso},51}^{-1/8}, \quad (14)$$

where  $t_j$  is the jet break time in the X-ray afterglow phase of GRBs, and  $n$  is the number density of the burst circumstance.

### 3. Results

The relations among the observational data of the prompt emission and afterglow in SGRBs, disk mass, and BH parameters are established by Equations (8-14). If the reasonable ranges of the BH parameters are given, the limits of the disk masses corresponding to the certain SGRBs can be resolved.

#### 3.1. Data of SGRBs

Berger (2014) mainly reviewed the progresses of SGRBs in the theories and observations, including the afterglow and host galaxy observations, the properties of the circumburst environments and their progenitors. There are 70 SGRBs with a substantial fraction of afterglow detections in the eight-year period from January 2005 to January 2013 (Berger 2014), with the addition of GRB 130603B (e.g., Berger et al. 2013; Tanvir et al. 2013), which is associated with a kilonova (Li & Paczyński 1998). As shown in Table 1 of Berger (2014), there are 27 SGRBs with the authentic X-ray detections and known redshifts discovered by *Swift* satellite except for GRB 050709 by HETE-2.

Moreover, we find 4 SGRBs with the X-ray detections and known redshifts triggered after GRB 130603B, i.e., GRBs 131001A, 140622A, 140903A, and 141212A, whose data are from the UK Swift Science Data Centre (Evans et al. 2009). So totally 31 SGRBs are listed in Table 1. For each SGRBs, we fit the photon index with the data of X-ray spectrum to deduce  $p$  (e.g., Zhang et al. 2006; Gao et al. 2013). Their durations  $T_{90}$ , redshifts  $z$ , gamma-ray fluences  $F_\gamma$  and X-ray fluxes at 11 hours since trigger  $F_X$  (11 hours), and the observed spectral index  $\beta$  are displayed. If we take  $\epsilon_e \sim 0.1$ ,  $\epsilon_B \sim 0.01$ ,  $Y \sim 0$ ,  $\eta = 0.3$ , and fitted  $p$  and given  $t_j$ , then  $E_{\gamma, \text{iso}}$ ,  $E_{k, \text{iso}}$ , and  $\theta_j$  can be solved, and we further obtain the ranges of the disk masses.

It is worth noting that the most difficult problem is the estimation of the jet opening angle  $\theta_j$  because of the faint and restricted observations of SGRB afterglows. So far there are three scenarios, i.e., (1) a few credible detections of jet break, such as in GRBs 051221A (Soderberg et al. 2006), 090426 (Nicuesa Guelbenzu et al. 2011), and 130603B (Fong & Berger 2013); (2) several meaningful lower limits on jet opening angles, such as in GRBs 050724 (Grupe et al. 2006), 111117A (Margutti et al. 2012), and 120804A (Berger et al. 2013); (3) no break in X-ray lightcurves of some SGRBs. We cite the data of the jet opening angles or their lower limits in the above references for former two cases as shown in Table 1. For the third scenario, we set the lower limit of  $\theta_j \gtrsim 0.05$  (Fong et al. 2012). For the last 4 SGRBs we collected, the jet break time,  $\sim 3.80_{-2.50}^{+0.00}$  ks, is found in GRB 140903, then we

can estimate the opening angle by Equation (14) with  $n = 0.01 \text{ cm}^{-3}$ , and the other three are set by the lower limit as discussed above.

### 3.2. Disk masses of SGRBs

Figure 1 shows the ranges of disk masses  $M_{\text{disk}}$  of the different SGRBs with the isotropic gamma-ray luminosity  $L_{\gamma,\text{iso}}$  for varying BH mass  $M_{\text{BH}}$  from  $2.7 M_{\odot}$  to  $10 M_{\odot}$  and BH spin  $a_*$  from 0 to 0.99. Three vertical lines correspond to  $M_{\text{disk}} = 0.2 M_{\odot}$ ,  $0.5 M_{\odot}$ , and  $1 M_{\odot}$ , respectively. It is seen that  $M_{\text{disk}}$  has a wide distribution, from about  $6 \times 10^{-4} M_{\odot}$  to about  $7.6 M_{\odot}$ , as well as shown in Table 1. The accretion rates corresponding to the minimal disk masses are checked, which are in the suitable ranges, i.e.,  $\dot{M}_{\text{ign}} < \dot{M} < \dot{M}_{\text{trap}}$ . There is no statistical correlation between the disk mass and gamma-ray isotropic luminosity, because the energy coming from the accretion powers all radiative processes of GRBs, mainly in gamma-ray and X-ray bands. The energies of the X-ray afterglows are frequently larger than those of prompt emission as displayed in Table 1. Obviously, the disk mass is primarily calculated by the output energy of GRBs, opening angle of the jet, and BH characteristics as shown in Equation (8). There exists a difference of several orders of magnitude between the minimal and maximal disk mass, which means that the BH characteristics are the major factors on the disk mass.

As shown in the figure, the maximal disk mass of GRBs 050724, 051221A, 070714B, 070809, 090426, 111117A, 120804A, and 131001A are larger than  $1 M_{\odot}$ , and that of most other SGRBs in our sample are larger than  $0.2 M_{\odot}$ , which indicates that the extreme BH spin parameters and small BH mass are required. In binary NS merger events, the BH mass is naturally less than the total mass of the binary, i.e.,  $\sim 4 M_{\odot}$ , which is described about  $\sim 2.7 M_{\odot}$  in further simulations. In BH-NS binaries, the BH is origin from its progenitor star, and its mass should also be a stellar-mass order, e.g.,  $\sim 10 M_{\odot}$ . Moreover, the BH spin parameters are also related to their progenitors. In some discussions (e.g., Lee et al. 2000b; Ruffert & Janka 2001), the rapidly rotating BHs ( $a_* \geq 0.5$ ) are inclined to exist in the SGRB centers in contrast to the BHs in the LGRB centers.

In order to embody the effects of the BH characteristics on the disk mass, Figure 2 displays the distributions of the disk masses  $M_{\text{disk}}$  for the different typical BH masses and spins, which are set to  $(M_{\text{BH}}/M_{\odot}, a_*) = (3, 0.5)$ ,  $(3, 0.9)$ ,  $(10, 0.5)$ , and  $(10, 0.9)$ , corresponding to (a-d), respectively. It is easy to find that the disk mass of most SGRBs are safe below  $0.2 - 0.4 M_{\odot}$ , and sporadic cases are beyond the limits, especially in the case of Figure 2(c). Additionally, by comparing these four cases, we notice that the spin parameters are more effective than the BH masses on the values of the disk masses. Even for the case of Figure



2(b), there still exists one SGRB, whose disk mass is larger than  $0.45 M_{\odot}$ . Those massive disks,  $\geq 1 M_{\odot}$ , may exist in the centers of collapsars, which are considered as the origin of LGRBs. Actually, Lazzati et al. (2010) proposed that the off-axis jets from collapsars could power SGRBs.

Three factors remind us that the results of the disk masses are the lower limits at the most, which are as follows. (1) We have to calculate the disk mass using the lower limit of  $\theta_j$  in most SGRBs as shown in Table 1. It is easily conceivable that the real requirements of the disk masses are much larger than the the present results if the precise value of  $\theta_j$  is considered. (2) Some powerful SGRBs with unknown redshift, such as GRBs 060121, 060313, and 111121A, shown in Table 1 of Berger (2014), may require more massive disk than SGRBs in our sample if they are also origin from the BH hyperaccretion systems. (3) The powerful X-ray flares have been extensively observed in the afterglow phase of GRBs, which are considered to originate from the re-ignition of the central engine (e.g., Liu et al. 2008; Luo et al. 2013; Hou et al. 2014). This means that the remanent matters from the massive disk are needed to maintain the explosion of X-ray flares. However, we use  $T_{90}$  to replace the duration of the activity of the central engine, which may generally enlarge the disk mass in the calculations. Although these influences and some uncertainties may exist, we consider that our results can still reflect the deficiency of the neutrino annihilation process to power SGRBs.

#### 4. Conclusions and discussion

The progenitor of SGRBs is considered to be a compact binaries merger event. After merger, a stellar-mass BH surrounded by an NDAF will be formed in the central SGRB and neutrino-antineutrino annihilation above the disk may power SGRBs. The total mass of two compact stars limits the mass of the system consisting of a BH and an NDAF. In this paper, we focus on a question, i.e., can annihilations of neutrinos from NDAFs owning such masses power all the observed SGRBs? The calculations show that the disk mass of a certain SGRB mainly depend on its output energy, jet opening angle, and central BH characteristics. Even for the extreme BH parameters, there still exist some SGRBs requiring the massive disks, which approach or exceed the limits in simulations.

Besides magnetar model, for BH hyperaccretion system, we suggest that there may exist an alternative magnetic origin of SGRBs, i.e., BZ process (e.g., Popham et al. 1999; Lee et al. 2000a,b; Di Matteo et al. 2002; Kawanaka et al. 2013) or episodic magnetic reconnection (Yuan & Zhang 2012), to replace neutrino annihilation. Kawanaka et al. (2013) presented that the luminosity powered by Poynting-dominated jet is more qualified for the requirement

of GRBs than neutrino pair annihilation. Yuan & Zhang (2012) investigated that the closed magnetic field lines continuously emerge out of the accretion flow. Since the shear and turbulent motion of the accretion flow, the line may form the flux rope. When a threshold is reached, the system loses its equilibrium and the flux rope is thrust outward, then an episodic jet occurs. This mechanism can also power enormous energy to trigger GRBs. In addition, if these magnetic origins really exist in the center of GRBs, the polarization effect should be observed in the prompt emission or afterglow of GRBs. Actually, the linear polarization in the afterglow of LGRB GRB 120308 has been detected (Mundell et al. 2013), which indicates that large-scale magnetic fields may be dominant in the GRB jets. But now we do not know whether the same situation exists in SGRBs.

Otherwise, there are some mechanisms, such as magnetic coupling from the BH horizon to the inner region of the disk (Li 2000), can effectively transfer the angular momentum and rotational energy of the BH to heat the inner region of the disk, then larger numbers of neutrinos radiate from the disk to produce the primordial fireball (e.g., Lei et al. 2009; Luo et al. 2013). Besides, the vertical advection (or convection) is considered to widely exist in the slim disks and NDAFs (Jiang et al. 2014; Liu et al. 2015), which is another possible mechanism to increase the neutrino emission rate. The scenario for NDAFs follows, the vertical advection (or convection) caused by magnetic buoyancy can much effectively transport energy to the disk surface, and also suppress the radial advection, thus the neutrino luminosity and annihilation luminosity are dramatically increased. This mechanism is conducive to achieve the energy requirement of GRBs.

We thank Yi-Zhong Fan, Fu-Wen Zhang and Xiao-Hong Zhao for beneficial discussion and the anonymous referee for very useful suggestions and comments. We acknowledge the use of the public data from the *Swift* archives. Our work also made use of data supplied by the UK Swift Science Data Centre at the University of Leicester. This work was supported by the National Basic Research Program of China (973 Program) under grant 2014CB845800, the National Natural Science Foundation of China under grants 11222328, 11233006, 11333004, 11373002, 11473022, U1231101, and U1331101, and the CAS Open Research Program of Key Laboratory for the Structure and Evolution of Celestial Objects under grants OP201305 and OP201403.

## REFERENCES

- Aloy, M. A., Janka, H.-T., & Müller, E. 2005, *A&A*, 436, 273
- Antoniadis, J., Freire, P. C. C., Wex, N., et al. 2013, *Science*, 340, 448
- Bardeen, J. M., Press, W. H., & Teukolsky, S. A. 1972, *ApJ*, 178, 347
- Berger, E. 2014, *ARA&A*, 52, 43
- Berger, E., Fong, W., & Chornock, R. 2013, *ApJ*, 774, L23
- Birkl, R., Aloy, M. A., Janka, H.-T., & Müller, E. 2007, *A&A*, 463, 51
- Blandford, R. D., & Znajek, R. L. 1977, *MNRAS*, 179, 433
- Chen, W. X., & Beloborodov, A. M. 2007, *ApJ*, 657, 383
- Demorest, P. B., Pennucci, T., Ransom, S. M., Roberts, M. S. E., & Hessels, J. W. T. 2010, *Nature*, 467, 1081
- De Pasquale, M., Schady, P., Kuin, N. P. M., et al. 2010, *ApJ*, 709, L146
- Di Matteo, T., Perna, R., & Narayan, R. 2002, *ApJ*, 579, 706
- Eichler, D., Livio, M., Piran, T., & Schramm, D. N. 1989, *Nature*, 340, 126
- Evans, P. A., Beardmore, A. P., Page, K. L., et al. 2009, *MNRAS*, 397, 1177
- Fan, Y., & Piran, T. 2006, *MNRAS*, 369, 197
- Fan, Y.-Z., & Wei, D.-M. 2011, *ApJ*, 739, 47
- Fong, W., & Berger, E. 2013, *ApJ*, 776, 18
- Fong, W., Berger, E., Margutti, R., et al. 2012, *ApJ*, 756, 189
- Frail, D. A., Kulkarni, S. R., Sari, R., et al. 2001, *ApJ*, 562, L55
- Fryer, C. L., Woosley, S. E., Herant, M., & Davies, M. B. 1999, *ApJ*, 520, 650
- Gao, H., Lei, W.-H., Zou, Y.-C., Wu, X.-F., & Zhang, B. 2013, *New A Rev.*, 57, 141
- Grupe, D., Burrows, D. N., Patel, S. K., et al. 2006, *ApJ*, 653, 462
- Gu, W.-M., Liu, T., & Lu, J.-F. 2006, *ApJ*, 643, L87

- Hou, S.-J., Liu, T., Gu, W.-M., et al. 2014, *ApJ*, 781, L19
- Janiuk, A., Mioduszewski, P., & Moscibrodzka, M. 2013, *ApJ*, 776, 105
- Jiang, Y.-F., Stone, J. M., & Davis, S. W. 2014, *ApJ*, 796, 106
- Kato, S., Fukue, J., & Mineshige, S. 2008, *Black-Hole Accretion Disks: Towards a New Paradigm* (Kyoto: Kyoto Univ. Press)
- Kawanaka, N., & Mineshige, S. 2007, *ApJ*, 662, 1156
- Kawanaka, N., Piran, T., & Krolik, J. H. 2013, *ApJ*, 766, 31
- Kohri, K., & Mineshige, S. 2002, *ApJ*, 577, 311
- Kohri, K., Narayan, R., & Piran, T. 2005, *ApJ*, 629, 341
- Kluźniak, W., & Lee, W. H. 1998, *ApJ*, 494, L53
- Kouveliotou, C., Meegan, C. A., Fishman, G. J., et al. 1993, *ApJ*, 413, L101
- Kovács, Z., Cheng, K. S., & Harko, T. 2011a, *MNRAS*, 411, 1503
- Kovács, Z., & Harko, T. 2011b, *MNRAS*, 417, 2330
- Lazzati, D., Morsony, B. J., & Begelman, M. C. 2010, *ApJ*, 717, 239
- Lee, H. K., Brown, G. E., & Wijers, R. A. M. J. 2000a, *ApJ*, 536, 416
- Lee, H. K., Wijers, R. A. M. J., & Brown, G. E. 2000b, *Phys. Rep.*, 325, 83
- Lee, W. H., & Kluźniak, W. 1999, *ApJ*, 526, 178
- Lee, W. H., Ramirez-Ruiz, E., & Page, D. 2005, *ApJ*, 632, 421
- Lei, W. H., Wang, D. X., Zhang, L., et al. 2009, *ApJ*, 700, 1970
- Leng, M., & Giannios, D. 2014, *MNRAS*, 445, L1
- Li, L.-X. 2000, *ApJ*, 533, L115
- Li, L.-X., & Paczyński, B. 1998, *ApJ*, 507, L59
- Liu, T., Gu, W.-M., Dai, Z.-G., & Lu, J.-F. 2010, *ApJ*, 709, 851
- Liu, T., Gu, W.-M., Kawanaka, N., & Li, A. 2015, *ApJ*, accepted, arXiv: 1503.04054

- Liu, T., Gu, W.-M., Xue, L., & Lu, J.-F. 2007, *ApJ*, 661, 1025
- Liu, T., Gu, W.-M., Xue, L., Weng, S.-S., & Lu, J.-F. 2008, *ApJ*, 676, 545
- Liu, T., Gu, W.-M., Xue, L., & Lu, J.-F. 2012a, *Ap&SS*, 337, 711
- Liu, T., Liang, E.-W., Gu, W.-M., et al. 2012b, *ApJ*, 760, 63
- Liu, T., Xue, L., Gu, W.-M., & Lu, J.-F. 2013, *ApJ*, 762, 102
- Liu, T., Yu, X.-F., Gu, W.-M., & Lu, J.-F. 2014, *ApJ*, 791, 69
- Lloyd-Ronning, N. M., & Zhang, B. 2004, *ApJ*, 613, 477
- Luo, Y., Gu, W.-M., Liu, T., & Lu, J.-F. 2013, *ApJ*, 773, 142
- Lü, H.-J., Zhang, B., Lei, W.-H., Li, Y., & Lasky, P. D. 2015, arXiv: 1501.02589
- MacFadyen, A. I., & Woosley, S. E. 1999, *ApJ*, 524, 262
- Nakar, E. 2007, *Phys. Rep.*, 442, 166
- Margutti, R., Berger, E., Fong, W., et al. 2012, *ApJ*, 756, 63
- Metzger, B. D., Giannios, D., Thompson, T. A., Bucciantini, N., & Quataert, E. 2011, *MNRAS*, 413, 2031
- Mészáros, P. 2002, *ARA&A*, 40, 137
- Mundell, C. G., Kopač, D., Arnold, D. M., et al. 2013, *Nature*, 504, 119
- Narayan, R., Paczyński, B., & Piran, T. 1992, *ApJ*, 395, L83
- Nicuesa Guelbenzu, A., Klose, S., Krühler, T., et al. 2012, *A&A*, 538, L7
- Nicuesa Guelbenzu, A., Klose, S., Rossi, A., et al. 2011, *A&A*, 531, L6
- Paczyński, B. 1991, *Acta Astronomica*, 41, 257
- Popham, R., Woosley, S. E., & Fryer, C. 1999, *ApJ*, 518, 356
- Rosswog, S., & Ramirez-Ruiz, E. 2002, *MNRAS*, 336, L7
- Rosswog, S., Ramirez-Ruiz, E., & Davies, M. B. 2003, *MNRAS*, 345, 1077
- Ruffert, M., & Janka, H.-T. 1998, *A&A*, 338, 535

- Ruffert, M., & Janka, H.-T. 2001, *A&A*, 380, 544
- Sari, R. 1997, *ApJ*, 489, L37
- Sari, R., Piran, T., & Halpern, J. P. 1999, *ApJ*, 519, L17
- Soderberg, A. M., Berger, E., Kasliwal, M., et al. 2006, *ApJ*, 650, 261
- Tanvir, N. R., Levan, A. J., Fruchter, A. S., et al. 2013, *Nature*, 500, 547
- Usov, V. V. 1992, *Nature*, 357, 472
- Woosley, S. E., & Bloom, J. S. 2006, *ARA&A*, 44, 507
- Xue, L., Liu, T., Gu, W.-M., & Lu, J.-F. 2013, *ApJS*, 207, 23
- Yuan, F., & Zhang, B. 2012, *ApJ*, 757, 56
- Zalamea, I., & Beloborodov, A. M. 2011, *MNRAS*, 410, 2302
- Zhang, B. 2006, *Nature*, 444, 1010
- Zhang, B., Fan, Y. Z., Dyks, J., et al. 2006, *ApJ*, 642, 354
- Zhang, B., Liang, E., Page, K. L., et al. 2007b, *ApJ*, 655, 989
- Zhang, B., & Mészáros, P. 2004, *International Journal of Modern Physics A*, 19, 2385
- Zhang, B., Zhang, B.-B., Liang, E.-W., et al. 2007a, *ApJ*, 655, L25

Table 1: Data of SGRBs

GRB	$T_{90}$ (s)	$z$	$F_\gamma$ ( $10^{-7}$ erg cm $^{-2}$ )	$F_X$ (11 hours) ( $10^{-14}$ erg cm $^{-2}$ s $^{-1}$ )	Photon index	$E_{\gamma,iso}^a$ ( $10^{51}$ ergs)	$E_{k,iso}^a$ ( $10^{51}$ ergs)	$\theta_j$ (rad)	$M_{disk}^b$ ( $M_\odot$ )
050509B	0.04	0.225	0.23	< 1.95	$1.6^{+0.5}_{-0.4}$	0.0027	0.055	$\gtrsim 0.05$	0.0006-0.028
050709	0.07	0.161	4.0	1.92	$\sim 2$	0.023	0.016	$\gtrsim 0.26$ (1)	0.003-0.14
050724	3	0.257	6.3	9.55	$1.68^{+0.15}_{-0.13}$	0.1	0.27	$\gtrsim 0.35$ (2)	0.084-3.93
051210	1.3	1.3	0.83	< 2.7	$2.78^{+0.48}_{-0.41}$	0.36	2.38	$\gtrsim 0.05$	0.016-0.76
051221A	1.4	0.5465	12	108	$2.09^{+0.10}_{-0.09}$	0.92	12.6	$\sim 0.12$ (3)	0.093-4.37
060502B	0.09	0.287	0.4	< 1.47	$2.15^{+1.07}_{-0.58}$	0.012	0.12	$\gtrsim 0.05$	0.0013-0.062
060801	0.5	1.130	0.81	< 0.98	$2.01^{+0.23}_{-0.26}$	0.27	0.71	$\gtrsim 0.05$	0.0063-0.30
061006	0.4	0.438	14	22.7	$1.86^{+0.26}_{-0.24}$	0.67	3.14	$\gtrsim 0.05$	0.013-0.59
061201	0.8	0.111	3.3	19.2	$1.54^{+0.17}_{-0.17}$	0.01	0.07	$\sim 0.017$ (4)	0.0014-0.067
061210	0.2	0.409	3.0	13.6	$2.60^{+1.92}_{-0.71}$	0.12	0.86	$\gtrsim 0.05$	0.0048-0.22
070429B	0.5	0.902	0.63	11.3	$2.69^{+1.18}_{-0.56}$	0.13	4.51	$\gtrsim 0.05$	0.013-0.63
070714B	2.0	0.923	7.2	6.30	$1.96^{+0.12}_{-0.15}$	1.61	2.32	$\gtrsim 0.05$	0.027-1.25
070724A	0.4	0.457	0.30	12.8	$1.46^{+0.36}_{-0.25}$	0.016	0.99	$\gtrsim 0.05$	0.007-0.33
070729	0.9	0.8	1.0	< 4.71	$1.5^{+0.6}_{-0.3}$	0.17	1.32	$\gtrsim 0.05$	0.012-0.54
070809	1.3	0.473	1.0	53.0	$1.39^{+0.14}_{-0.12}$	0.056	3.91	$\gtrsim 0.05$	0.024-1.15
071227	1.8	0.381	2.2	3.20	$2.19^{+0.41}_{-0.35}$	0.08	0.25	$\gtrsim 0.05$	0.01-0.47
080905A	1.0	0.122	1.4	< 6.7	$1.54^{+0.22}_{-0.44}$	0.005	0.024	$\gtrsim 0.05$	0.0027-0.13
090426	1.2	2.609	1.8	26.3	$2.03^{+0.16}_{-0.15}$	2.84	135	$\sim 0.07$ (5)	0.093-4.35
090510	0.3	0.903	3.4	5.04	$1.70^{+0.12}_{-0.12}$	0.73	3.07	$\sim 0.017$ (4)	0.0035-0.17
090515	0.04	0.403	0.21	< 8.43	$2.73^{+1.20}_{-0.77}$	0.008	0.62	$\gtrsim 0.05$	0.0016-0.075
100117A	0.3	0.915	0.93	< 2.50	$2.74^{+0.36}_{-0.31}$	0.20	1.10	$\gtrsim 0.05$	0.0057-0.27
100206A	0.1	0.408	1.4	< 1.07	$2.0^{+0.8}_{-0.7}$	0.058	0.073	$\gtrsim 0.05$	0.0013-0.062
100625A	0.3	0.453	2.3	0.395	$2.3^{+0.5}_{-0.3}$	0.12	0.093	$\gtrsim 0.05$	0.003-0.14
101219A	0.6	0.718	4.6	2.00	$1.44^{+0.27}_{-0.25}$	0.62	0.45	$\gtrsim 0.05$	0.008-0.38
111117A	0.5	1.3	1.4	3.21	$2.10^{+0.39}_{-0.32}$	0.62	3.77	0.105 (6)	0.023-1.06
120804A	0.81	1.3	8.8	58.6	$2.10^{+0.22}_{-0.14}$	3.88	56.9	$\gtrsim 0.19$ (7)	0.16-7.59
130603B	0.18	0.356	6.3	60.0	$2.00^{+0.14}_{-0.13}$	0.20	2.80	$\sim 0.07$ (8)	0.01-0.48
131001A	1.54	0.717	2.8	14.7	$1.91^{+0.18}_{-0.18}$	0.37	5.41	$\gtrsim 0.05$	0.029-1.37
140622A	0.13	0.959	0.27	17.0	$1.55^{+0.67}_{-0.28}$	0.065	9.77	$\gtrsim 0.05$	0.0087-0.41
140903A	0.30	0.351	1.4	124.7	$1.59^{+0.22}_{-0.20}$	0.043	6.15	0.023 (9)	0.0067-0.31
141212A	0.30	0.596	0.72	2.50	$2.0^{+0.8}_{-0.5}$	0.066	0.38	$\gtrsim 0.05$	0.0039-0.18

Notes:

<sup>a</sup> The parameters are calculated by Equation (12) with  $\epsilon_e \sim 0.1$ ,  $\epsilon_B \sim 0.01$ , and  $Y \sim 0$ .

<sup>b</sup> The ranges of  $M_{disk}$  are estimated by Equation (8) with  $\eta = 0.3$ , varying  $M_{BH}$  from  $2.7 M_\odot$  to  $10 M_\odot$ , and  $a_*$  from 0 to 0.99.

References:

(1) Berger 2014; (2) Grupe et al. 2006; (3) Soderberg et al. 2006; (4) De Pasquale et al. 2010; Nicuesa Guelbenzu et al. 2012; (5) Nicuesa Guelbenzu et al. 2011; (6) Margutti et al. 2012; (7) Berger et al. 2013; (8) Fong & Berger 2013; (9) The opening angle of GRB 140903A is determined by Equation (14) with the data from the UK Swift Science Data Centre (Evans et al. 2009) and  $n \sim 0.01$  cm $^{-3}$ .

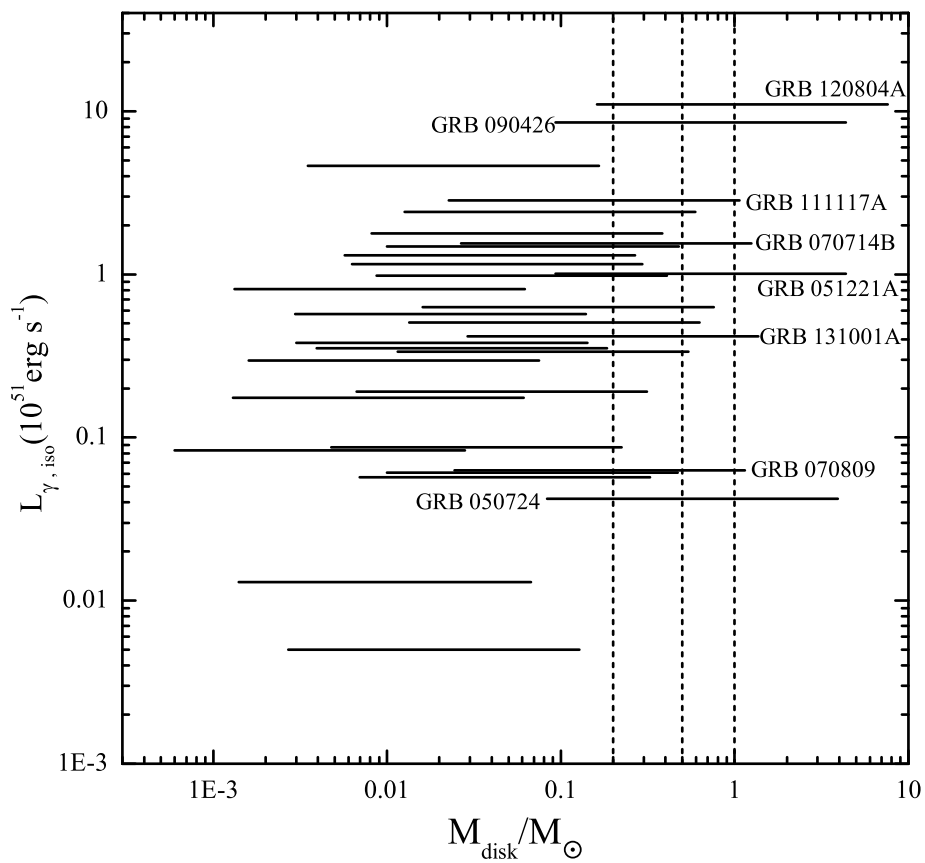


Fig. 1.— Ranges of disk masses  $M_{\text{disk}}$  of different SGRBs with isotropic gamma-ray luminosity  $L_{\gamma, \text{iso}}$  for varying BH mass  $M_{\text{BH}}$  from  $2.7 M_{\odot}$  to  $10 M_{\odot}$  and BH spin  $a_*$  from 0 to 0.99. Three vertical lines correspond to  $M_{\text{disk}} = 0.2 M_{\odot}$ ,  $0.5 M_{\odot}$ , and  $1 M_{\odot}$ , respectively.



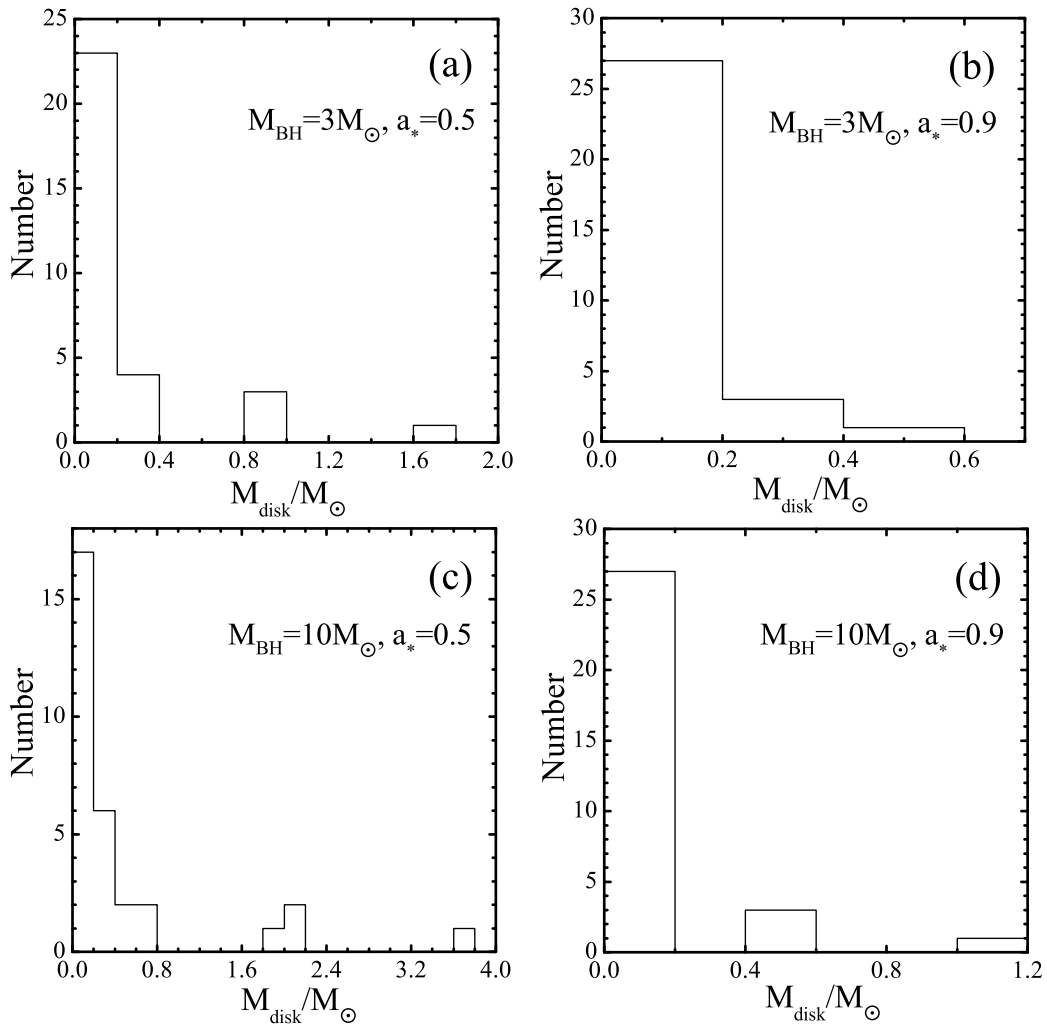


Fig. 2.— Distributions of the disk masses  $M_{\text{disk}}$  for different typical BH masses and spins.